# Structures of small Au clusters on MgO(001) studied by density-functional calculations

R. Ferrando,[1] G. Barcaro,[2] and A. Fortunelli[2]
[1]*Dipartimento di Fisica and CNISM, Via Dodecaneso 33, Genova, I-16146, Italy*
[2]*Molecular Modeling Laboratory, IPCF/CNR, via G. Moruzzi 1, Pisa, I-56124, Italy*
(Received 25 September 2010; published 27 January 2011)

The structure of Au clusters adsorbed on MgO(001) is studied by density-functional calculations. The results of two different exchange-correlation functionals, the local density approximation (LDA) and the Perdew–Burke–Ernzerhof (PBE) functionals, are compared. The size range $11 \leqslant N \leqslant 24$ atoms is considered. It is shown that a complex competition among a variety of structural motifs takes place. These motifs comprise two-dimensional leaflets, open cages, tetrahedral cages, and compact three-dimensional structures. Both functionals predict qualitatively the same kind of behavior with increasing cluster size, with morphology transitions from leaflets to open cages and finally to compact structures, together with a narrow range, around $N = 20$, in which tetrahedral cages are dominant. However, there are quantitative differences about the sizes of the crossover, which occurs at smaller sizes according to the LDA functional with respect to the PBE functional. This result is consistent with the fact that the LDA functional overestimates metallic bonding in Au, whereas the PBE functional underestimates it.

DOI: 10.1103/PhysRevB.83.045418 PACS number(s): 68.43.Hn, 61.46.Bc, 61.46.Df, 68.43.Bc

## I. INTRODUCTION

Gold nanoparticles[1,2] have attracted a great deal of interest in the last decades for several reasons, ranging from the discovery of the catalytic activity of small aggregates[3] to a variety of unexpected geometries and behaviors,[4–26] for both gas-phase and surface-supported nanoparticles.

Among the motifs that have been found for gold nanoparticles we can mention gas-phase amorphous structures,[4,27] two-dimensional (2D) leaflets,[28,29] tetrahedra,[6] and fullerenelike cages.[9–11] Supported clusters may present an even wider variety of structures, which are dictated by the interplay between gold-gold[2] and gold-substrate[30] interactions.

A recent example of peculiar supported structures is related to gold clusters adsorbed on the defect-free surface of MgO(001).[24] The MgO(001) surface has been one of the most widely used substrates for model catalysts.[31,32] It is a surface of square symmetry, presenting a checkerboard of alternating Mg and O atoms. When gold atoms are deposited on it, they preferentially adsorb on oxygen sites.[33] Recent density-functional (DF) calculations[24] have singled out a new family of Au/MgO(001) clusters, the *open pyramidal hollow cages*, which have no counterpart in gas-phase clusters. In these cages, all gold atoms are on the cluster surface, since their basis (i.e., the part of the pyramid which is in contact with the substrate) is reduced to atoms along the perimeter only. According to DF calculations employing the gradient-corrected Perdew–Burke–Ernzerhof (PBE) exchange-correlation (xc) functional,[34] these cages show a remarkable energetic stability in the size range between 25 and 40 atoms, with magic sizes for $N = 25$ and $N = 32$ atoms. In this size range, the calculations show that open pyramidal hollow cages are lower in energy than compact structures and gas-phase cages for all sizes.

This energetic stability was attributed to the interplay of two effects.[24]

The first effect is the tendency of Au to form closely packed monolayers in undercoordinated systems.[35] This is related to the fact that this metal loses only a small part of its binding energy in passing from the bulk 12-coordinated-monolayer situation to the closely packed 6-coordinated monolayers. This leads to planar structures for small gas-phase clusters[5] and to the reconstruction of low-index Au surfaces, and it stabilizes the compact facets of supported pyramidal cages.

The second effect is related to the peculiar character of the Au/MgO interaction. These interactions are of directional and strongly many-body character.[36] In fact, an isolated Au atom on the defect-free MgO(001) surface interacts appreciably with the oxygen ions also via a chemical bond component. However, the strength of this interaction drops rapidly with Au coordination, because of the competition with metal-metal bonds. Therefore, atoms in clusters interact with the substrate mainly by polarization forces with a strong metal-on-top effect. The metal-on-top effect is an increased metal-surface interaction due to the presence of metal atoms on top of the atom directly in contact with the substrate.[36] Because of that, for highly coordinated Au atoms it is not favorable to be in contact with the MgO surface. On the opposite, the interaction of low-coordinated atoms is much more favorable, especially if enhanced by the metal-on-top effect. These features are well met by the open pyramidal hollow cages, which have low-coordinated perimetral basal atoms with a proper set of on-top neighbors. These predictions were confirmed by calculation of vibrational modes[26] and using other gradient-corrected xc functionals.[24,37]

In this paper we extend the study of Au/MgO(001) clusters to a different size range, the interval $11 \leqslant N \leqslant 24$. In this interval, a competition of open pyramidal cages with other structural motifs, which are not favorable for $N \geqslant 25$, is expected. As we shall see in the following, these motifs comprise 2D leaflets, tetrahedral cages (as found for neutral $Au_{20}$ by Yoon and Landman[16]), and a new type of open cages, which are not pyramidal. Two different xc functionals are employed in this study. The first is the gradient-corrected PBE functional, the second is the local density approximation (LDA). The choice of two functionals is due to that fact that they have opposite tendencies for what concerns Au-Au interactions, since the PBE functional is underbinding and the

 

LDA is overbinding: the cohesive energy of bulk gold is 3.10 and 4.34 eV according to the PBE functional and the LDA, respectively, to be compared with an experimental value of 3.81 eV. For this reason, the PBE functional is expected to be biased in favor of planar and cage cluster structures against compact structures, while the LDA is expected to be biased in the opposite direction. The comparison of the results of the PBE and LDA functionals is thus likely to be meaningful for bracketing the structural trends of Au/MgO(001) clusters. We note however that the PBE functional has been found to be in better agreement with the experiments on gas-phase gold clusters than the LDA[7,38,39] and that the experimental diffusion barrier of single gold atoms on MgO(001) is more closely (even though not perfectly) reproduced by the PBE functional.[33,40]

In Ref. 24, the MgO substrate was kept rigid, with Mg and O atoms fixed at their experimental distance. Here we perform calculations also by allowing the topmost layer of the substrate to relax, in order to check the effects of a nonrigid substrate. Even though the relaxation of the substrate is not expected to play a major role, our aim is to quantitatively assess its effect on the different cluster structures.

The paper is organized as follows. Section II deals with the computational methodology, Sec. III reports the results, and Sec. IV contains discussion and conclusions.

## II. METHODS

Our computational methodology comprises two steps.[24,41,42]

The first is devoted to the construction of a vast database of structures belonging to the different motifs. Compact structures are searched for by means of a global optimization procedure[43] within an empirical potential model. This model comprises metal-metal and metal-substrate interactions. The metal-metal interactions are modeled by a force field derived within the second-moment approximation to the tight-binding model.[44–46] The metal-substrate interaction is a potential energy surface which is fitted on DF calculations.[43,47] This empirical potential has been tested in Ref. 43, where it has been shown that it is possible to reproduce structures in agreement with the existing experimental observations[32,48] related to large clusters (containg a few hundred atoms or more), in which compact structures clearly prevail. Cage structures are built up either by accommodating on the substrate the gas-phase structures or by building up open cages (see the following). All structures are locally relaxed at the DF level. For 2D leaflets and for cages, several shapes are considered. Two-dimensional leaflets are accommodated in both vertical and horizontal orientations with respect to the substrate.

The second step is the DF calculations, which are carried out using the PWscf (plane-wave self-consistent field) code,[49] with PBE or LDA xc functionals and ultrasoft pseudopotentials. In the majority of the calculations, the substrate has been kept rigid. In rigid-substrate calculations, the MgO(001) surface is modeled by a two-layer slab. Depending on the cluster structure and size, different slabs are employed in order to ensure a sufficient distance between clusters in periodic images on the $x$-$y$ plane. These slabs contain either 36 Mg and 36 O atoms ($6 \times 6$ and $9 \times 4$ cells) or 35 Mg and 35 O atoms ($7 \times 5$ cell), fixed in the lattice positions of the MgO bulk structure. Separation between periodic images along the $z$ directions has been varied to reach convergence of the energy differences reported in the following. In calculations in which the topmost MgO layer is allowed to relax, three MgO layers are used, with the bottom two layers kept frozen.

The kinetic energy cutoff is 40 Ry for the energy and 160 Ry for the density for all calculations. Checks have been made on selected structures by increasing energy cutoffs and finding that energy differences between isomers do not change by more that 0.002 eV. Because of the large unit cells, eigenvalues and eigenvectors of the Kohn–Sham Hamiltonian are only evaluated at the $\Gamma$ point. A Gaussian smearing technique[50] (with a smearing parameter of 0.002 Ry) is applied.

## III. RESULTS

### A. Competing structural motifs

In the size range $11 \leqslant N \leqslant 24$ several structural motifs are in competition. Representative clusters of these motifs are shown in Figs. 1 and 2. These motifs are the following.

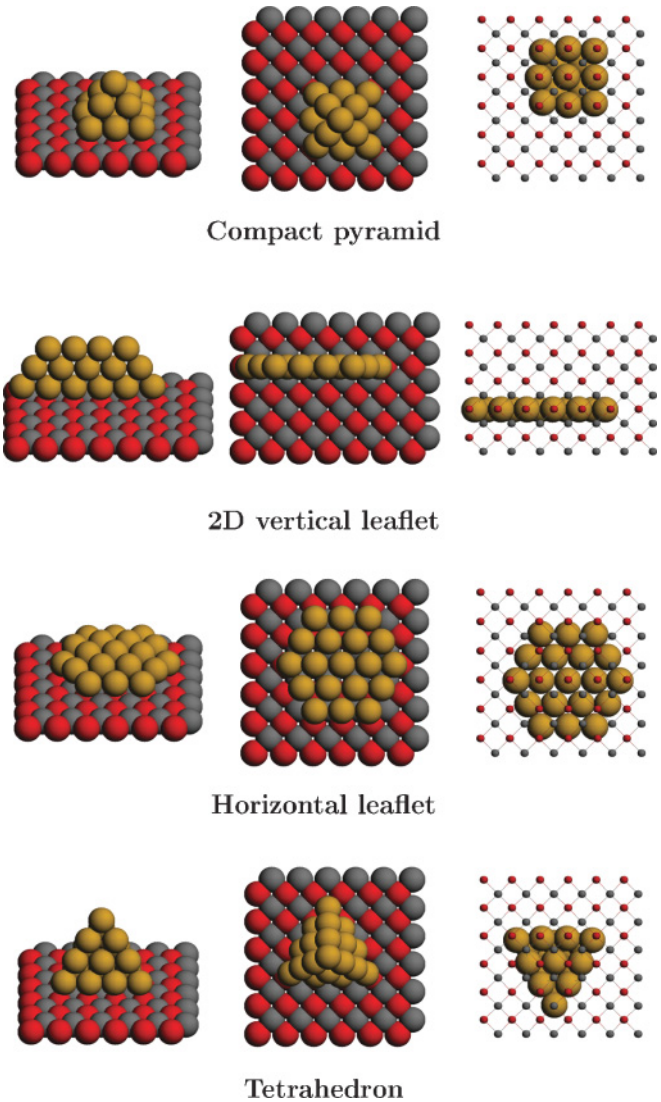


FIG. 1. (Color online) Competing structural motifs in the size range $11 \leqslant n \leqslant 24$.

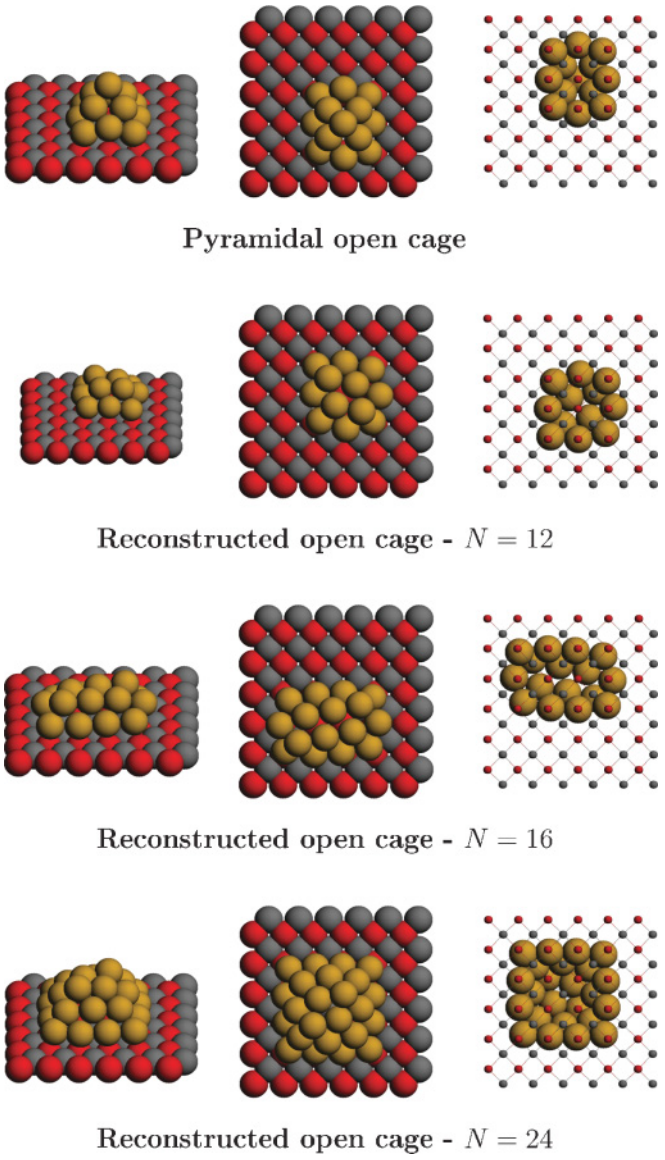


FIG. 2. (Color online) Other competing structural motifs in the size range $11 \leqslant n \leqslant 24$.

*Compact pyramids.* These structures continue the cube-on-cube fcc(001) epitaxy of the substrate. These pyramids are named compact because they contain *inner atoms*; i.e., atoms that are not at the interface with vacuum. Compact pyramids can have either a square basis or a rectangular basis. Square pyramids are complete for $N = 14$ and $N = 30$ ($3 \times 3$ and $4 \times 4$ basis, respectively). A complete rectangular pyramid ($4 \times 3$ basis) is complete for $N = 20$. For sizes other than 14 and 20, compact pyramids present either truncations at the vertex or at the basal corners or even overhangs.[41,51]

*2D vertical leaflets*. These 2D structures are stabilized by the tendency of gold to form 2D structures in the gas phase[5] and by the metal-on-top effect.[36] Two-dimensional vertical leaflets were found to be the most favorable structures for small clusters adsorbed on flat MgO, for sizes up to $Au_7$, by gradient-corrected DF calculations.[20] In general, these leaflets tend to be more favorable for sizes at which it is possible to build up structures with three (or four, when size increases) atomic rows in which the number of atoms decreases by one going from the lowest row to the highest one. In this size range, this is possible for $N = 12$, 15, 18, 19, 21,22, and 24.

*Horizontal leaflets.* These structures are leaflets, made by a single gold layer, but they are not really 2D, because they bulge so that central atoms stay higher than periphery atoms. For example, for $N = 19$, the $z$ coordinates of the central and of the periphery vertex atoms differ by 0.9 and 0.6 Å according to PBE and LDA calculations, respectively. Favorable sizes for these structures are $N = 13$ and 19.

*Tetrahedra.* Tetrahedral structures lean on the substrate with a triangular facet. A complete tetrahedron is found for $N = 20$. Incomplete tetrahedra are obtained by erasing vertex atoms.

*Pyramidal open cages.* These structures are completely empty and can be seen also as folded leaflets. Complete pyramids are found for sizes 13 and 25 (square basis) and $N = 18$ (rectangular basis). Incomplete pyramidal open cages are obtained by eliminating basal corner atoms or vertex atoms.

*Reconstructed open cages.* These structures are obtained by erasing vertex atoms of pyramidal open cages and locally relaxing the structure, which undergoes a transformation of its top facet as shown in Fig. 3. This transformation is energetically favorable because new gold-gold nearest-neighbor bonds are formed, at the expense of some distortion of the structure. The reconstruction leads to the appearance of local fivefold symmetry points, with pentagonal rings appearing at the top of the structure. Complete reconstructed open cages are found for $N = 12$, 16, and 24. Favorable incomplete structures of this motif are obtained by eliminating atoms at the basal corners.

### B. Size range $11 \leqslant N \leqslant 16$

The results obtained in this size range are reported in Table I.

According to the PBE functional, 2D vertical structures are dominant for all sizes, followed by pyramidal or reconstructed open cages. These cages are in close competition with vertical leaflets for sizes 13, 14, and 16. Sizes 13 and 16 are in fact magic sizes for the open cages. Horizontal leaflets and compact pyramids are much higher in energy. An icosahedral cage is found for $N = 11$, but is unfavorable compared to pyramidal or reconstructed cages.

The LDA predicts a rather different behavior. Pyramidal or reconstructed open cages are the lowest in energy, with the

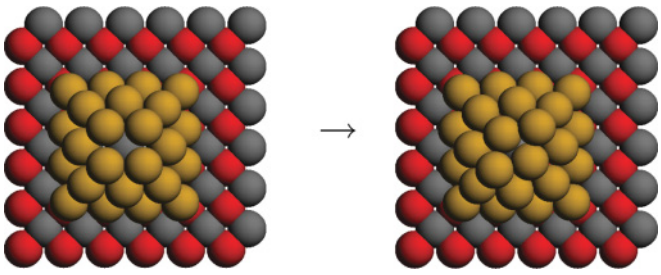

FIG. 3. (Color online) Reconstruction of open pyramidal cages. In the figure, an open pyramidal cage of 25 atoms is truncated at its top vertex, so as to expose a square facet which, on local relaxation, undergoes a transformation to a rhombic shape. In this way a new gold-gold nearest-neighbor bond is formed.

TABLE I. Energetics of the structural motifs for $11 \leqslant N \leqslant 16$. Energy differences (in eV) from the lowest isomer are reported.

| Size | Structure | PBE | LDA |
|---|---|---|---|
| 11 | 2D vertical | 0.000 | 0.396 |
| | Pyramidal open cage | 0.547 | 0.085 |
| | Reconstructed open cage | 0.582 | 0.000 |
| | Horizontal leaflet | 0.701 | 0.275 |
| | Icosahedral cage | 0.895 | 0.607 |
| | Square pyramid | 1.222 | 0.455 |
| 12 | 2D vertical | 0.000 | 0.643 |
| | Pyramidal open cage | 0.370 | 0.000 |
| | Reconstructed open cage | 0.470 | 0.074 |
| | Square pyramid | 0.953 | 0.415 |
| 13 | 2D vertical | 0.000 | 1.159 |
| | Pyramidal open cage | 0.079 | 0.000 |
| | Horizontal leaflet | 0.698 | 0.684 |
| | Square pyramid | 0.776 | 0.146 |
| 14 | 2D vertical | 0.000 | 0.936 |
| | Pyramidal open cage | 0.152 | 0.000 |
| | Square pyramid | 0.944 | 0.047 |
| 15 | 2D vertical | 0.000 | 0.791 |
| | Pyramidal open cage | 0.924 | 0.137 |
| | Square pyramid | 0.981 | 0.000 |
| 16 | 2D vertical | 0.000 | 0.791 |
| | Reconstructed open cage | 0.167 | 0.000 |
| | Pyramidal open cage | 0.215 | 0.287 |
| | Square pyramid | 0.225 | 0.041 |

exception of $N = 15$, for which the compact pyramid prevails. Compact pyramids are, however, in close competition with the cages from size 13 on. Horizontal leaflets are more favorable than vertical leaflets, but they are in competition with the best structures only for $N = 11$, and then they become clearly unfavorable.

### C. Size range $17 \leqslant N \leqslant 20$

The results obtained in this size range are reported in Table II.

In this size interval tetrahedral structures come into play.[16,30] These are the lowest in energy for sizes 18, 19, and 20 for both PBE and LDA calculations. For size 17 the tetrahedral structure does not prevail, but is nevertheless in close competition with the best structures. This is therefore the size range in which the lowest-energy structures of supported clusters resemble more closely gas-phase structures.[6,7]

PBE and LDA calculations agree also in predicting that pyramidal or reconstructed open cages are in close competition with the tetrahedal structures, being slightly lower in energy for $N = 17$ and slightly higher in the other cases.

By analogy with what is found for $11 \leqslant N \leqslant 16$, PBE and LDA calculations disagree in singling out the third competing motif besides tetrahedra and open cages, which is the 2D vertical leaflet for PBE and the compact pyramid for LDA, respectively. Horizontal leaflets are never favorable, not even at their magic number 19.

TABLE II. Energetics of the structural motifs for $17 \leqslant N \leqslant 20$. Energy differences (in eV) from the lowest isomer are reported.

| Size | Structure | PBE | LDA |
|---|---|---|---|
| 17 | 2D vertical | 0.000 | 1.615 |
| | Pyramidal open cage | 0.125 | 0.000 |
| | Tetrahedron | 0.199 | 0.123 |
| | Rectangular pyramid | 0.963 | 0.424 |
| 18 | Tetrahedron | 0.000 | 0.000 |
| | Pyramidal open cage | 0.096 | 0.204 |
| | 2D vertical | 0.118 | 1.848 |
| | Rectangular pyramid | 1.315 | 0.683 |
| 19 | Tetrahedron | 0.000 | 0.000 |
| | 2D vertical | 0.234 | 2.473 |
| | Pyramidal open cage | 0.352 | 0.269 |
| | Horizontal leaflet | 0.445 | 0.615 |
| | Rectangular pyramid | 1.024 | 0.154 |
| 20 | Tetrahedron | 0.000 | 0.000 |
| | Reconstructed open cage | 0.265 | 0.150 |
| | 2D vertical | 0.665 | |
| | Rectangular pyramid | 1.211 | 0.029 |

### D. Size range $21 \leqslant N \leqslant 24$

The results obtained in this size range are reported in Table III.

In this size range, open cages dominate, especially in their reconstructed form. According to PBE calculations, they are the lowest in energy for all sizes, whereas according to LDA they prevail for sizes 22 and 23, being however close to the lowest-energy structures (compact pyramids) for sizes 21 and 24. In summary, PBE calculations predict a neat prevalence of open cages, while LDA calculations predict a close competition between open cages and compact structures. Vertical

TABLE III. Energetics of the structural motifs for $21 \leqslant N \leqslant 24$. Energy differences (in eV) from the lowest isomer are reported.

| Size | Structure | PBE | LDA |
|---|---|---|---|
| 21 | Reconstructed open cage | 0.000 | 0.025 |
| | Pyramidal open cage | 0.079 | 0.284 |
| | 2D vertical | 0.173 | |
| | Tetrahedron | 0.225 | 0.538 |
| | Rectangular pyramid | 0.895 | 0.000 |
| 22 | Reconstructed open cage | 0.000 | 0.000 |
| | Pyramidal open cage | 0.049 | 0.241 |
| | 2D vertical | 0.608 | |
| | Tetrahedron | 0.634 | 0.976 |
| | Square pyramid | 0.873 | 1.343 |
| | Rectangular pyramid | 0.946 | 0.408 |
| 23 | Reconstructed open cage | 0.000 | 0.000 |
| | Pyramidal open cage | 0.075 | 0.196 |
| | 2D vertical | 0.422 | |
| | Tetrahedron | 0.758 | 0.973 |
| | Square pyramid | 0.865 | 0.113 |
| 24 | Reconstructed open cage | 0.000 | 0.223 |
| | Pyramidal open cage | 0.088 | 0.437 |
| | Square pyramid | 0.448 | 0.000 |

leaflets are still in competition for $N = 21$ according to PBE calculations, but they become unfavorable with increasing size. We also note that for $N > 24$, LDA calculations predict a clear transition to compact structures. Pyramidal open cages are in competition with compact structures only at the magic sizes $N = 25$ and 32. On the contrary, according to PBE calculations the size range $25 \leqslant N \leqslant 40$ is dominated by open cages,[24] the transition to compact structures taking place above size 40.

### E. Effects of substrate relaxation

Since MgO is a quite rigid crystal,[31,32] we expect that surface relaxation should not play a major role. However, it is interesting to check to what extent substrate relaxation can affect the results presented in the previous sections. To this purpose, we have performed calculations including substrate relaxation for a few selected sizes. In these calculations, the topmost layer of the MgO slab is left free to relax, while the layers below are kept fixed as before.

Our calculations confirm that the effect of surface relaxation is small, so that it does not alter the qualitative picture emerging from rigid-substrate calculations. For PBE calculations, the energy differences between isomers are altered by less than 0.1 eV, and this is not sufficient to change their energetic ordering. For LDA calculations, the effect of substrate relaxation is somewhat more important. For example, at $N = 11$ LDA calculations with rigid substrate predict that the pyramidal cage is the lowest in energy and that the reconstructed cage is almost degenerate but higher by 0.006 eV. After substrate relaxation, the reconstructed cage prevails by 0.085 eV. At $N = 32$, the difference between the compact structure and the pyramidal open cage decreases from 0.35 to 0.16 eV.

As an overall trend, the inclusion of substrate relaxation tends to favor cage structures compared to compact structures, because the former present generally a larger number of atoms in contact with the substrate that can take advantage from the relaxation.

## IV. DISCUSSION AND CONCLUSIONS

We have shown that small Au clusters on MgO present a surprising variety of structures in competition with each other whose energetic stability is size dependent and also xc functional dependent.

At first glance the predictions of PBE and LDA calculations seem to be in apparent disagreement. In fact, only for five sizes over 14 do they predict the same structures as being the lowest in energy: for sizes 18, 19, and 20, the tetrahedral structure; for sizes 22 and 23, the reconstructed open cage. However, a closer scrutiny reveals intrinsic similarities. In fact, both PBE and LDA calculations predict the same overall trend, with the same kind of structural transitions with increasing size: from planar structures to (pyramidal and reconstructed) open cages and finally to compact structures, with an interval dominated by tetrahedra for sizes 18–20. The difference is simply that structural transitions are displaced to higher sizes for the PBE functional with respect to the LDA. Therefore, for what concerns the qualitative structural behavior of Au/MgO clusters, the disagreement between LDA and PBE predictions is more apparent than real. PBE and LDA calculations actually disagree for what concerns leaflets and compact structures (by analogy with what occurs in the gas phase[8]). According to LDA calculations, leaflets are never in competition with the best structures in the size range above 10 atoms, while compact structures are already low in energy. Moreover, horizontal leaflets are somewhat more stable than vertical ones. On the contrary, according to PBE calculations, compact structures become competitive for sizes larger than 24, while vertical leaflets are dominant up to size 17. In any case, both LDA and PBE calculations agree in predicting a good energetic stability for open cages and tetrahedra. These differences between PBE and LDA calculations can be rationalized in terms of the tendency to underbind and overbind, respectively, the Au-Au bond.

The inclusion of substrate relaxation does not seem to be important for this system, as it leads to rather small changes in the energy differences between isomers. These changes should anyway tend to favor cage structures over compact ones.

We remark that our calculations do not include the effect of temperature. For sizes at which isomers are in close competition, say within 0.1–0.2 eV, entropic effects, due to vibrational entropy,[26] might become important and reverse their ordering.

Finally, it should be noted that the nucleation of gold nanoparticles on MgO often occurs at defects, especially at step edges. Nucleation at steps may alter cluster shapes, even though cage structures are likely to be less rigid and to better adapt their relaxation to the defect geometry. However this issue has to be investigated in detail and will be the subject of further work.

## ACKNOWLEDGMENTS

R.F. acknowledges support from the Italian MIUR for PRIN Project 2007LN873M_003. A.F. acknowledges support from the FP7 of the European Community within the SEPON Project (ERC-AG). The authors acknowledge support from CINECA and CNR-INFM for the project "Properties of Exotic Phases of Metal-on-Oxide Nanodots."

[1] M.-C. Daniel and D. Astruc, Chem. Rev. **104**, 293 (2004).
[2] P. Pyykkö, Angew. Chem. Intl. Ed. **43**, 4412 (2004).
[3] H. Haruta, Catal. Today **36**, 153 (1997).
[4] I. L. Garzon, K. Michaelian, M. R. Beltran, A. Posada-Amarillas, P. Ordejon, E. Artacho, D. Sanchez-Portal, and J. M. Soler, Phys. Rev. Lett. **81**, 1600 (1998).
[5] M. Moseler, H. Häkkinen, and U. Landman, Phys. Rev. Lett. **89**, 176103 (2002).
[6] J. Li, X. Li, H.-J. Zhai, and L.-S. Wang, Science **299**, 864 (2003).
[7] P. Gruene, D. M. Rayner, B. Redlich, A. F. G. van der Meer, J. T. Lyon, G. Meijer, and A. Fielicke, Science **321**, 674 (2008).
[8] E. Aprà, R. Ferrando, and A. Fortunelli, Phys. Rev. B **73**, 205414 (2006).
[9] M. P. Johansson, D. Sundholm, and J. Vaara, Angew. Chem. Intl. Ed. **43**, 2678 (2004).

[10]X. Gu, M. Ji, S. H. Wei, and X. G. Gong, Phys. Rev. B **70**, 205401 (2004).
[11]Q. Sun, Q. Wang, P. Jena, R. Note, J.-Z. Yu, and Y. Kawazoe, Phys. Rev. B **70**, 245411 (2004).
[12]F. Baletto and R. Ferrando, Rev. Mod. Phys. **77**, 371 (2005).
[13]S. Bulusu, X. Li, L.-S. Wang, and X. C. Zeng, Proc. Natl. Acad. Sci. USA **103**, 1330 (2006).
[14]B. Yoon, H. Hakkinen, U. Landman, A. S. Worz, J. M. Antonietti, S. Abbet, K. Judai, and U. Heiz, Science **307**, 403 (2005).
[15]B. Yoon, P. Koskinen, B. Huber, O. Kostko, B. von Issendorff, H. Hakkinen, M. Moseler, and U. Landman, ChemPhysChem **8**, 157 (2007).
[16]B. Yoon and U. Landman, Phys. Rev. Lett. **100**, 056102 (2008).
[17]A. F. Jalbout, F. F. Contreras-Torres, L. A. Perez, and I. L. Garzon, J. Phys. Chem. A **112**, 353 (2008).
[18]J. L. Elechiguerra, J. Reyes-Gasga, and M. José-Yacaman, J. Mater. Chem. **16**, 3906 (2006).
[19]Y. Gao and X. C. Zeng, J. Am. Chem. Soc. **127**, 3698 (2005).
[20]L. M. Molina and J. A. Alonso, J. Phys. Chem. C **111**, 6668 (2007).
[21]D. X. Tian and J. J. Zhao, J. Phys. Chem. A **112**, 3141 (2008).
[22]A. J. Karttunen, M. Linnolahti, T. A. Pakkanen, and P. Pyykkö, Chem. Commun. **4**, 465 (2008).
[23]G. Barcaro and A. Fortunelli, Chem. Phys. Lett. **457**, 143 (2008).
[24]R. Ferrando, G. Barcaro, and A. Fortunelli, Phys. Rev. Lett. **102**, 216102 (2009).
[25]H. S. Nam, N. M. Hwang, B. D. Yu, and J. K. Yoon, Phys. Rev. Lett. **89**, 275502 (2002).
[26]W. Fa, J. Zhou, X. Li, and J. Dong, J. Phys. Chem. C **114**, 13035 (2010).
[27]E. Aprà, F. Baletto, R. Ferrando, and A. Fortunelli, Phys. Rev. Lett. **93**, 065502 (2004).
[28]G. Bravo-Perez, I. L. Garzón, and O. Novaro, Chem. Phys. Lett. **313**, 655 (1999).
[29]V. Bonačič-Koutecky, J. Burda, R. Mitrič, M. Ge, G. Zampella, and P. Fantucci, J. Chem. Phys. **117**, 3120 (2002).
[30]G. Barcaro and A. Fortunelli, J. Phys. Chem. B **110**, 21021 (2006).
[31]C. R. Henry, Surf. Sci. Rep. **31**, 235 (1998).
[32]C. R. Henry, Prog. Surf. Sci. **80**, 92 (2005).
[33]G. Barcaro and A. Fortunelli, New J. Phys. **9**, 22 (2007).
[34]J. P. Perdew, K. Burke, and M. Ernzerhof, Phys. Rev. Lett. **77**, 3865 (1996).
[35]S. Olivier, R. Conte, and A. Fortunelli, Phys. Rev. B **77**, 054104 (2008).
[36]G. Barcaro and A. Fortunelli, J. Chem. Theory Comput. **1**, 972 (2005).
[37]See EPAPS Document No. [E-PRLTAO-102-020924] for details on the methodology and for auxiliary results.
[38]E. M. Fernandez, J. M. Soler, and L. C. Balbas, Phys. Rev. B **73**, 235433 (2006).
[39]B. S. de Bas, M. J. Ford, and M. B. Cortie, J. Mol. Struct.: THEOCHEM **686**, 193 (2004).
[40]M. Yulikov, M. Sterrer, T. Risse, and H. J. Freund, Surf. Sci. **603**, 1622 (2009).
[41]G. Barcaro, A. Fortunelli, G. Rossi, F. Nita, and R. Ferrando, Phys. Rev. Lett. **98**, 156101 (2007).
[42]R. Ferrando, A. Fortunelli, and R. L. Johnston, Phys. Chem. Chem. Phys. **10**, 640 (2008).
[43]R. Ferrando, G. Rossi, A. C. Levi, Z. Kuntová, F. Nita, G. Barcaro, A. Fortunelli, A. Jelea, C. Mottet, and J. Goniakowski, J. Chem. Phys. **130**, 174702 (2009).
[44]F. Cyrot-Lackmann and F. Ducastelle, Phys. Rev. B **4**, 2406 (1971).
[45]R. P. Gupta, Phys. Rev. B **23**, 6265 (1981).
[46]V. Rosato, M. Guillope, and B. Legrand, Philos. Mag. A **59**, 321 (1989).
[47]W. Vervisch, C. Mottet, and J. Goniakowski, Phys. Rev. B **65**, 245411 (2002).
[48]B. Pauwels, G. Van Tendeloo, W. Bouwen, L. T. Kuhn, P. Lievens, H. Lei, and M. Hou, Phys. Rev. B **62**, 10383 (2000).
[49]P. Giannozzi, S. Baroni, N. Bonini, M. Calandra, R. Car, C. Cavazzoni, D. Ceresoli, G. L. Chiarotti, M. Cococcioni, I. Dabo *et al.*, J. Phys.: Condens. Matter **21**, 395502 (2009).
[50]C. Elsässer, M. Fähnle, C. T. Chan, and K. M. Ho, Phys. Rev. B **49**, 13975 (1994).
[51]L. M. Molina and B. Hammer, Appl. Catal. A **291**, 21 (2005).